

RESISTANCE OF REINFORCED CONCRETE BRIDGE COLUMNS SUBJECTED TO BLAST LOADS

CHRISTOPHER EAMON, *e-mail: eamon@eng.wayne.edu*

AHMAD ASLENDI

Wayne State University, Dept. of Civil & Env. Engineering, Detroit, MI, USA

Abstract: A large strain, large displacement finite element model that allows element separation and failure is constructed and validated based on existing results of reinforced concrete columns subjected to blast loads. In this approach, concrete is represented with the Johnson-Holmquist-Cook model while a plastic-kinematic relationship describes steel behavior. The model is used to predict the capacity of typical reinforced concrete bridge columns to resist an assumed blast load scenario, where changes in concrete strength, steel reinforcement ratio, and axial force on the column are considered. The effectiveness of a method of column protection is investigated, where existing columns are wrapped with a relatively inexpensive steel fiber reinforced polymer (SFRP) jacket. It was found that the use of SFRP can significantly enhance the resistance of the columns.

Keywords: concrete, columns, bridges, finite element analysis, blast, explosive load

1. Introduction

Bridge design in the United States is primarily governed by standards set by the American Association of State Highway and Transportation Officials LRFD Bridge Design Specifications [1]. Although the LRFD Specifications recognize the importance of blast loading, these standards do not contain corresponding design provisions in detail. For example, AASHTO notes that the blast force (BL) is governed by the size, shape, type, and location of the explosive charge as well as other parameters, but suggests that specific design criteria are to be determined by the bridge owner. Although various elements of a bridge structure may be damaged due to blast load, including the deck, girders, piers, abutments, and even foundation components, of particular importance are the bridge columns (piers), which are highly exposed and if severely damaged, may lead to the progressive collapse of the entire structure [2].

Over the last decade, a relatively small but increasing body of research has been conducted to better understand the vulnerability and behavior of bridge structures exposed to blasts. Some of this work considered the entire structure [3, 4], although most efforts studied individual components such as decks, girders, and columns.

Studies focused on columns include that of Williamson [5, 6] and Williams [7, 8, 9], who identified various parameters that influence the performance of concrete columns subjected to blast loading. Major parameters were splice location, cross-section shape and size, and transverse reinforcement type and spacing. It was found that square columns performed better than circular, and that continuous spiral reinforcement performed better than tied. Son [10] and Yi [11] studied column failures, and found that multiple modes are possible, including crushing or shearing of the column base; fracturing reinforcement; surface spalling; and plastic hinge formation. Others explored retrofit and protection options [12, 13, 14], and found that steel and composite jacketing could enhance shear capacity and reduce concrete crushing. Additional work suggested that concrete-filled steel tubes could exhibit satisfactory performance against blast loads [15, 16, 17].

As summarized above, although experimental as well as analytical research has been conducted to characterize blast load effects on bridge columns and some design recommendations to resist blast have been proposed, the response of these critical bridge components under blast threats remains uncertain. Some reasons for this lack of knowledge are that blast experiments are relatively expensive to conduct, few test facilities are available, and highly refined models are very computationally demanding. Moreover, without detailed descriptions of experimental work, which are often limited in the published literature due to security concerns, numerical work is challenging to validate. Therefore, the development of a reasonably simple but accurate model that can be used to predict the response of bridge columns under blast threats is desirable, as is a better understanding of the behavior of these elements as well as the effectiveness of protective measures. To address these issues, in this study, a numerical (finite element) model is developed and validated based on existing results of blast experiments. The model is used to predict the response of typical bridge columns to various blast scenarios, where changes in concrete strength, steel reinforcement ratio, axial load, and blast charge weight are considered in a parametric analysis. Moreover, the effectiveness of a common method of retrofit is investigated, where existing columns are wrapped with a relatively inexpensive steel fiber reinforced polymer (SFRP) jacket.

2. Columns considered

The columns considered represent the supporting elements of the central pier of a multi-span structure. Many such designs are possible, and as only the column elements are considered in this study, the details of the surrounding structure are not critical. However, it was assumed that the columns are joined together by a column cap above, upon which the bridge girders rest, and below by a continuous beam that may form part of the roadway barrier, leaving 3 m of unsupported column length. Although columns satisfy AASHTO LRFD requirements, designing these elements to the minimum strength standards required results in cross-sections that are much smaller than those used in practice. Therefore, based on a survey of bridge column designs by state Departments of Transportation in the United States [5], the column cross-sections were increased in size to 760 mm square, as shown in Figure 1. These short (slenderness ratio L/r of 14), tied columns were reinforced with 24 longitudinal bars and #4 ties spaced at 150 mm on center, with a clear cover of 50 mm. Depending on the design case considered, longitudinal bar diameters were taken as 19 mm (#6 US), 25 mm (#8 US), or 35 mm (#11 US), with corresponding reinforcement ratios ρ of 0.012, 0.021, and 0.042. Reinforcing steel was taken as ASTM A615 Grade 60, with 420 MPa nominal yield strength. Concrete compressive strength was varied from $f'_c = 21$ to 55 MPa.

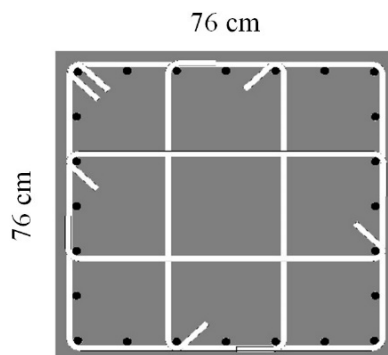


Fig. 1. Column cross-section

To increase column resistance to blast load, the use of a SFRP retrofit reinforcement was explored. The SFRP sheet is composed of uni-directional ultra-high strength steel wires which can be wrapped around a column and secured to the concrete with resin, in a manner similar to that used for externally-bonded FRP fabric [18]. Such wrapping systems are generally used to enhance the confinement strength of existing columns and thereby increase axial load capacity. However, as relatively inexpensive and practical means of protecting existing bridge columns from blast threats are limited, the potential effectiveness of using SFRP for this purpose was examined. Although more traditional composite wraps are available, such as those composed of carbon fiber, the SFRP alternative is relatively inexpensive (similar in price to glass FRP) as well as ductile. In this study, the SFRP sheet properties (1.2 mm thick) are taken as 985 MPa for yield stress and 66.1 GPa for elastic modulus (in the strong direction; stiffness and strength are practically zero in the weak direction), based on commercially available products [18]. In this study, it is assumed that two SFRP sheets are applied to the column in perpendicular directions; i.e. one oriented transversely as expected, and another layer oriented longitudinally.

3. Material models

Columns were modeled with a large strain, large displacement Lagrangian finite element procedure allowing element separation, disintegration, and contact, using an explicit solution algorithm as implemented in LS-DYNA [19]. Concrete behavior was represented with the Johnson-Holmquist- Cook (JHC) model, which was formulated for concrete when subjected to large strains and high strain rates and pressure [20]. In the JHC approach, effective concrete strength is given as a function of pressure, strain rate, and damage, where pressure is expressed as a function of volumetric strain and includes the effect of crushing. Material damage is accumulated as a function of plastic volumetric strain, equivalent plastic strain, and pressure, while the cohesive component of the equivalent strength is degraded as damage accumulates. The (external) pressure- (internal) stress relationship is given as:

$$\sigma^* = [A(1-D) + BP^{*N}][1 - \ln(\dot{\epsilon}^*)] \tag{1}$$

This is expressed in terms of normalized equivalent stress σ^* ($\sigma^* = \sigma / f'c$) and normalized pressure P^* ($P^* = P / f'c$), where σ is the actual equivalent stress; $f'c$ the uniaxial compressive stress of concrete; P the actual pressure; and $\dot{\epsilon}^*$ the dimensionless strain rate ($\dot{\epsilon}^* = \dot{\epsilon} / \dot{\epsilon}_0$), while $\dot{\epsilon}$ is the actual strain rate and $\dot{\epsilon}_0$ the reference strain rate, taken as $1.0s^{-1}$. Material constants are A , the normalized cohesive strength; B , the normalized pressure hardening coefficient; N , the pressure hardening exponent; C , the strain rate coefficient; and $SMAX$, the normalized maximum strength of the material. To evaluate fracture, the model accumulates damage (D) from equivalent plastic strain and plastic volumetric strain, and this expression is written as:

$$D = \sum [\Delta\epsilon + \Delta\mu_p / D_1 (P^* + T^*)^{D_2}] \tag{2}$$

where: D_1 and D_2 are material damage constants; $\Delta\epsilon_p$ and $\Delta\mu_p$ are the equivalent plastic strain and plastic volumetric strains, respectively; and T^* is the normalized maximum tensile hydrostatic pressure ($T^* = T / f'c$), while T is the maximum tensile hydrostatic pressure. An additional damage constant, $EFMIN$, is included to provide a minimum plastic strain necessary to initiate damage from fracture. In the model, the hydrostatic pressure-volume relationship is composed of a linear elastic region, which governs when $P \leq P_{crush}$; a linear transition region representing compression of the air voids producing plastic volumetric strain, where

$P_{crush} \leq P \leq P_{lock}$; and a nonlinear third region where no air voids are within the concrete at a pressure of P_{lock} , and is governed by:

$$P = K1\bar{u} + K2\bar{u}^2 + K3\bar{u}^3 \quad (3)$$

In these relationships, P_{crush} is a function of the elastic bulk modulus K and volumetric strain μ_{crush} , as measured from a uniaxial compression test: $K = P_{crush}/\mu_{crush}$. In Eq. 3, $K1$, $K2$, and $K3$ are material constants, and \bar{u} is the modified volumetric strain which is a function of the volumetric strain corresponding to P_{lock} , μ_{lock} : $\bar{u} = \bar{u} - \bar{u}_{lock} / 1 + \bar{u}_{lock}$. In this study, material constants are based on concrete test results reported in the literature [20, 5], and are given in Table 1.

Reinforcing steel is modeled with an elastic-plastic kinematic model, where yield stress is taken as 450 MPa and post-yield modulus is conservatively taken as zero. The SFRP sheet is modeled similarly, but with yield stress of 985 MPa.

Table 1. Concrete model parameters

Parameter	Value	Parameter	Value
A	0.79	T	1.7, 3.5, 4.6 MPa*
B	1.6	P_{crush}	6.9, 13.8, 18.4 MPa*
C	0.007	u_{crush}	4.2, 8.4, 11.2×10^{-4}
N	0.61	P_{lock}	800 MPa
S_{MAX}	7.0	u_{lock}	0.1
$D1$	0.04	$K1$	85000 MPa
$D2$	1.0	$K2$	-171000 MPa
EF_{MIN}	0.01	$K3$	208000 MPa

*For concrete strengths of 21, 41, and 55 MPa, respectively.

4. Blast load model

Once detonated, an explosive load forms a propagating shock wave that decays until ambient pressure is returned. The shock wave represents compression of the air, resulting in a dramatic increase in pressure above atmospheric, the peak overpressure. In this study, blast load is modeled using the CONWEP formulation [21], algorithms for which are a numerical implementation of the work of Kingery and Bulmash [22], in which blast loads of various charges were empirically modeled for use in a Modified Friedlander's Equation (for the positive region):

$$P(t) = P_0 \left(1 - \frac{(t-t_a)}{t_d} \right) \exp \left(-b \frac{(t-t_a)}{t_d} \right) \quad (4)$$

In this expression, P_0 is the peak overpressure; t_a the time of arrival, and t_d the duration of the positive phase, and b a decay coefficient. The shock wave will be reflected by objects in its path, including the ground surface. This reflected wave, if it strikes a structural element, could result in a significant pressure increase beyond the direct blast. Reflected blast overpressure is a function of the angle of shock wave incidence as well as time. Combining the reflected blast overpressure as well as the incident overpressure results in:

$$P(t) = P_r(t) \cos^2 \theta + P_{so}(t) (1 + \cos^2 \theta - 2 \cos \theta) \quad (5)$$

In this formulation, θ is the angle of incidence between the blast and the reflecting surface; $P_r(t)$ is the reflected blast pressure, which is computed from Eq. (1) with $P_o=P_r$; and $P_s(t)$ is the side-on (i.e. direct) overpressure, computed from Eq (1) with $P_o = P_{so}$. In this study, as detailed below, the charge is placed relatively close to the ground, and as such, a hemispherical surface burst is assumed; i.e. reflected shock waves are included.

5. Finite element model

Initially, concrete was modeled with solid hexahedral elements with edge size ranging from approximately 1.4 – 2.5 cm, resulting in a model size of approximately 171,000 elements. However, it was found that similar capacity results could be obtained with a much coarser mesh, with edge sizes of 9.5 cm for elements close to the charge where most cracks appear, and edge sizes of 9.5 cm square and 38 cm high for elements away from the charge. This resulted in only 1090 elements, with a corresponding large decrease in solution time. This more coarse model loses effectiveness for predicting detailed crack patterns, however. Although concrete elements are softened with damage accumulation based on the material model described above, an element is assumed to be disintegrated, and thus deleted from the model, when maximum principal compressive strain reaches 0.003. Once deleted, a contact surface is generated upon the faces of the remaining exposed elements, allowing for arbitrary contact and separation to model debris collision.

Reinforcing bars were explicitly modeled with beam elements. The bars are assumed to be fully bonded to the concrete with no slip, and thus share nodes with the concrete elements. To prevent possible penetration of a bar element into a concrete element during the large deformations associated with the blast, a contact surface was used between the bars and surrounding concrete (solid) elements that enforces this constraint.

For cases when the SFRP retrofit jacket was considered, it was similarly found that a relatively coarse mesh did not lead to significant differences in column capacity as compared to a much finer mesh. Correspondingly, the SFRP was modeled with shell elements with dimensions of 7.5 by 250 cm, resulting in 100 elements per column face. As similar to the beam elements used to model the reinforcing bars, a contact surface is used to prevent the SFRP shell elements from penetrating concrete elements. SFRP elements are assumed to be destroyed (and deleted from the model) at a maximum principal strain of 0.021.

Nodes at the column base were fully constrained, while an axial load was placed on the column to represent the bridge superstructure weight. Conservatively, no additional lateral constraints were placed at the top of the column. The axial load was varied from 100 to 285 kN, depending on the column considered. The upper range of this load represents the reaction of a column due to the service dead load of a two-lane, continuous girder highway bridge of 10.6 m overall width with each span 15 m long and supporting a 200 mm thick reinforced concrete deck. As it is conservative to apply lower values of axial force on the column when exposed to blast, lower axial load levels were also considered for different column configurations. These values were generated by maintaining the same proportion of axial load to column nominal capacity, and may be thought to represent smaller bridge geometries. Due to the low probability of simultaneous occurrence of a heavy vehicle on the bridge and a blast load, conservatively, no live load is included. The blast initiation point is placed 50 mm above the lower support of the column and 400 mm from the column face, to represent a charge placed on the ground adjacent to the column.

6. Validation

The finite element analysis (FEA) approach described above was used to model columns exposed to blast load as described by Williamson (2011). These columns are similar in dimensions, construction, and blast load application as those chosen for consideration in this study and as described above, with cross-sectional dimensions and reinforcement as shown in Figure 2, with 24 longitudinal bars of 19 mm diameter (#6 US). The test column has $f'_c = 28$ MPa and no axial load was applied, with a fixed base and free column top. Results are shown in Figure 2, which compares the deformed shape of the column after the blast to that of the model. Major cracks predicted in the model are highlighted. As shown, good agreement exists between the experimental and model results in terms of overall deformed shape, spalled regions, as well as crack pattern. As shown near the lower right side of the column (Figure 2), the angle of deformation of the longitudinal reinforcing bars also appears very similar. The only quantitative datum available is maximum column displacement, which occurs at the top of the column. At the completion of the blast duration (approximately 5–6 ms), the test column had a maximum displacement of 6.6 cm, whereas the analysis prediction was 7.1 cm. Based on these results, the authors considered the model sufficiently accurate for the purposes of this study.

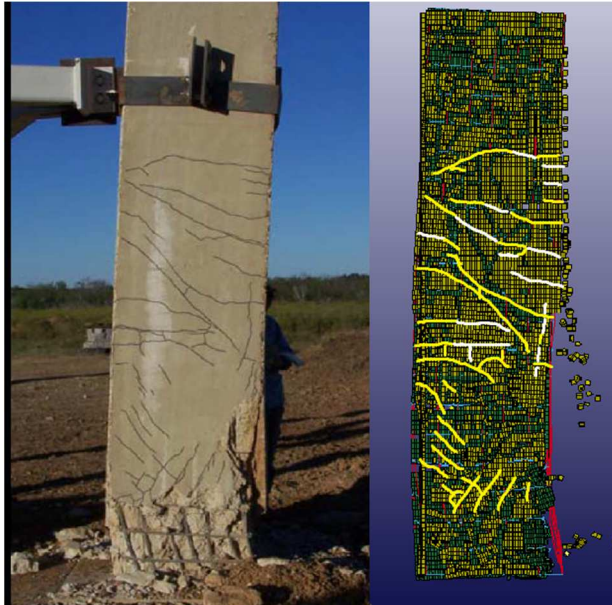


Fig. 2. Experimental and FEA results

7. Results

Using the FEA model above, a blast analysis was conducted for columns with different combinations of concrete strength, axial load, longitudinal steel, and charge weight. In addition to applying the service dead load on the column (*SDL*), to examine the effect of axial load magnitude, another series of analyses were conducted where the column was loaded to its maximum nominal capacity, representing the highest possible axial load. In the analysis, for a particular column design, the minimum charge weight was determined that would damage the column to an extent such that it could no longer support the applied axial load. As shown in Figure 3, a reasonably linear relationship exists between concrete strength and blast load

resistance in most cases. For columns loaded with service load, doubling concrete strength approximately doubles blast resistance. As shown in Figure 4, column resistance to blast load is approximately linearly related to longitudinal steel reinforcing ratio as well. However, results are less sensitive to steel content than concrete strength, where increasing reinforcement ratio by a factor of approximately 3.5 results in a range of resistance increases from about 1.3-2.0.

Also shown on Figures 3 and 4 is the column response when SFRP sheets are applied. For the column considered ($f_c = 41$ MPa with $\rho = 0.042$), applying one layer of SFRP (in each direction) increased blast capacity from 0.45 to 0.60 (equivalent kg of TNT) under service dead load, and from 0.85 to 0.95 with maximum axial load, representing an increase in capacity of 33% and 12%, respectively. However, additional layers resulted in relatively minor increases in capacity; applying as many as 10 layers provided an increase in capacity to 0.65 (44% increase) and 1.10 kg (30% increase) of TNT, respectively.

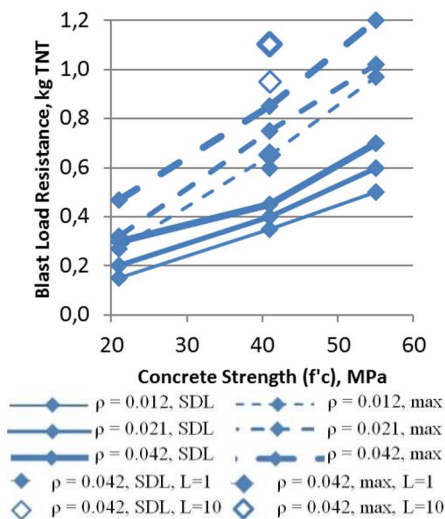


Fig. 3. Effect of compressive strength

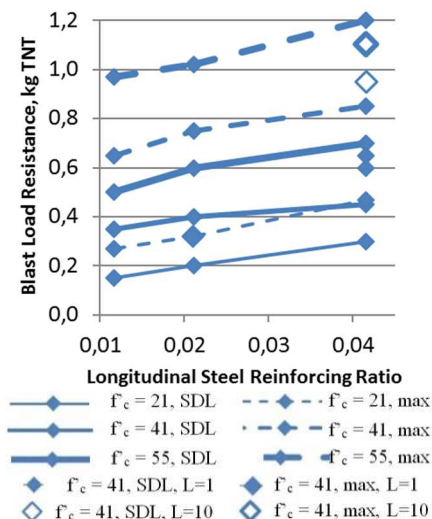


Fig. 4. Effect of reinforcement ratio

8. Conclusion

In this study, a reasonably simple and accurate model that can be used to predict the response of bridge structures under blast threats was developed and used to determine the blast resistance of bridge pier columns. Using a Johnson-Holmquist-Cook model for concrete behavior and a plastic-kinematic relationship for steel within a finite element approach that allows for element contact and disintegration, it was found that a relatively coarse mesh can be used to determine blast capacity. Using the validated model, the effect of concrete strength, steel reinforcement ratio, axial load, and SFRP sheets for retrofit on blast resistance were investigated. It was found that a reasonably linear relationship exists between concrete strength and blast load resistance in most cases, while capacity is less sensitive to steel content, where increasing reinforcement ratio by a factor of approximately 3.5 results in a range of resistance increases from about 1.3–2.0. It was further found that SFRP may represent a relatively inexpensive retrofit for blast protection, where applying 1 SFRP layer increased blast capacity by 33% under service dead load. However, additional layers resulted in relatively minor increases in capacity.

References

1. American Association of State and Highway Transportation Officials.: AASHTO LRFD Bridge Design Specifications, 2014.
2. Yi Z., Agrawal A., Ettouney M. Alampalli S.: Blast load effects on highway bridges. I: modeling and blast load effects. *ASCE Journal of Bridge Engineering*, 2013.
3. Zhu H, Zhang X, Li Y.: Analysis of the synergetic effects of blast wave and fragment on concrete bridges. *Chinese Society of Theoretical and Applied Mechanics*, 2013.
4. Winget D., Marchand, K., Williamson E.: Analysis and design of critical bridges subjected to blast loads. *ASCE Journal of Bridge Engineering*, 2005.
5. Williamson E., Oguzhan B., Carrie D., Williams G.: Performance of bridge columns subjected to blast loads. I: experimental program. *ASCE Journal of Bridge Engineering*, 2011.
6. Williamson E., Oguzhan B., Carrie D., Williams G.: performance of bridge columns subjected to blast loads. II: results and recommendations. *ASCE Journal of Bridge Engineering*, 2011.
7. Williams G., Holland, C. Williamson, E., Bayrak, O., Marchand, K., Ray, J.: Blast-resistant highway bridges: design and detailing guidelines. WITPress, Ashurst Lodge, Ashurst, Southampton, United Kingdom, 2008.
8. Williams, G.: Analysis and response mechanisms of blast loaded reinforced concrete columns. Ph.D. dissertation, Univ. of Texas at Austin, Austin, TX., 2009.
9. Williams, G. Daniel and Williamson Eric B.: Response of reinforced concrete bridge columns subjected to blast loads. *ASCE Journal of Bridge Engineering*, 2011.
10. Son J., Lee, H-J.: Performance of cable-stayed bridge pylons subjected to blast loading. Elsevier Ltd, Kidlington, Oxford, United Kingdom, 2011.
11. Yi Z., Agrawal A., Ettouney M. Alampalli S.: Blast load effects on highway bridges. II: failure modes and multihazard correlations. *ASCE Journal of Bridge Engineering*, 2013.
12. Fujikura S., Bruneau, M.: Experimental investigation of seismically resistant bridge piers under blast loading. *ASCE Journal of Bridge Engineering*, 2011.
13. Malvar L., Crawford J., Morrill K.: Use of composites to resist blast. *ASCE Journal of Bridge Engineering*, 2007.
14. Heffernan P., Wight R., Erki M.-A.: Research on the Use of FRP for critical load-bearing infrastructure in conflict zones. *ASCE Journal of Bridge Engineering*, 2011.
15. Marchand K., Williamson E., Winget D.: Analysis of blast loads on bridge substructures. WITPress, Ashurst Lodge, Ashurst, Southampton, United Kingdom, 2004.
16. Rutner M., Astaneh-asl, A. Son, J.: Blast resistant performance of steel and composite bridge piers. ETH Honggerberg, Zurich, Switzerland, 2006.
17. Fujikura S., Bruneau M., Lopez-Garcia D.: Experimental investigation of multihazard resistant bridge piers having concrete-filled steel tube under blast loading. *ASCE Journal of Bridge Engineering*, 2008.
18. Hardwire Armor Systems: Hardwire tapes. Pocomoke City MD. <https://www.hardwirellc.com>, accessed 2017.
19. Livermore Software Technology Corporation.: LS-DYNA keyword user's manual, version 971, Livermore, CA., 2013.
20. Holmquist T, Johnson G, Cook W.: A computational constitutive model for concrete subjected to large strains, high strain rates, and high pressures. Proc., 14th Int. Symp. on Ballistics, American Defense Preparedness Association, 1993.
21. Hyde D.: User's Guide for Microcomputer Program CONWEP, Applications of TM 5-855-1, Fundamentals of Protective Design for Conventional Weapons. SL-88-1, U.S. Army Corps of Engineers Waterways Experiment Station Instruction, Vicksburg, MS, 1988.
22. Kingery, C, Bulmash, G.: Air-Blast Parameters from TNT Spherical Air Burst and Hemispherical Surface Burst. ARBRL-TR-02555, U.S. Army Ballistic Research Laboratory, Aberdeen Proving Ground, MD, 1984.